

Improvement of source and wind field input of atmospheric dispersion model by assimilation of concentration measurements: Method and applications in idealized settings

Ivan V. Kovalets ^{*a)}, Vasso Tsiouri ^{b)}, Spyros Andronopoulos ^{b)}, John G. Bartzis ^{c)}

^{a)} Institute of Mathematical Machine and System Problems NAS of Ukraine, prosp. Glushkova 42, 03187, Kiev, Ukraine

^{b)} Environmental Research Laboratory, Institute of Nuclear Technology and Radiation Protection, NCSR 'Demokritos', Aghia Paraskevi, Greece

^{c)} Department of Engineering and Management of Energy Resources, University of Western Macedonia, Kozani, Greece

Abstract

The problem of correcting the pollutant source emission rate and the wind velocity field inputs in a puff atmospheric dispersion model by data assimilation of concentration measurements has been considered. Variational approach to data assimilation has been used, in which the specified cost function is minimized with respect to source strength and/or wind field. The analyzed wind field satisfied the constraints derived from the conditions of mass conservation and linearized flow equations for perturbations from the first guess wind field. 'Identical twin' numerical experiments have been performed for the validation of the method. The first-guess estimation errors of source emission rate and wind field were set to a factor of up to 10 and up to 6 m/s respectively. The calculations results showed that in most studied cases an improvement of vector wind difference (VWD) error by about 0.7-1 m/s could be achieved. The resulting normalized mean square error (NMSE) of concentration field was also reduced significantly.

Keywords data assimilation, meteorological modelling, inverse problems, emergency response.

1. Introduction

Atmospheric Dispersion Models (ADMs) are frequently used in Emergency Response Systems (ERSs) for the prediction of pollutants dispersion following accidental releases (e.g., in EU nuclear emergency response system RODOS, [1]). The quality of the ADMs results obviously depends both on the complexity of the ADM and on accuracy of the input data. In cases of nuclear emergencies the most important errors are related to the estimation of source emission rate and to the input meteorological data, [2]. Input data quality can often be improved by assimilation of available measurements (e.g., [3]). Variational approach is one of the most popular data assimilation methods [4], since it allows improving the quality of the predicted results by adjusting the input data and simultaneously keeping physical balance between calculated fields.

A lot of work has been devoted to improvement of source function estimation by variational assimilation of the concentration measurements. In the vast majority of works the meteorological parameters had been fixed (excellent review for such works concerning global emission modelling can be found in [5] and examples of other works dealing with accidental release modelling are [6],[7],[8]). This allowed reducing data assimilation problem to linear regression.

Since meteorological data can also significantly influence results of the ADMs prediction, the problem of improving the meteorological input data by assimilating meteorological measurements in the Meteorological Pre-Processors (MPP) of the ERSs has been also considered in several works (e.g., [18], [20]). However, concentration measurements around the point of release also contain information about the local meteorological fields and potentially could be used for the improvement of the meteorological data through data assimilation.

An attempt to improve the wind field information with concentration measurements was firstly performed in [21]. That work considered a very different in comparison to the present work atmospheric dispersion problem - modelling of the planetary ozone distribution. The problem of estimation of one-dimensional wind field from concentration measurements in Eulerian ADM has been solved with the extended Kalman Filtering approach (EKF), while source function was assumed to be known. In the work [22] the same idea was used in context of data assimilation in regional atmospheric dispersion problem (2D flow had been considered). In that work source function again was assumed to be known and ensemble Kalman Filtering method was used together with Eulerian ADM. In the work [7], the problem of combined adjustment of wind vector and source rate following the accidental release of contaminant was considered. However it was limited to the case of constant wind and source in space and in time.

The objective of the present paper is to develop a data assimilation methodology for improving the wind field (variable in space) and source function information with the use of concentration measurements in a Lagrangian-Eulerian (puff) atmospheric dispersion model. The motivation for the model choice is that in present

time puff models are widely used in emergency response systems and in other studies of atmospheric dispersion. For instance, RIMPUFF model, [9], and puff version of DIPCOT ADM, [10], are used in ERSs DERMA, [11], and RODOS, [1], CALPUFF model [12], which is recommended by Environmental Protection Agency of USA for environmental risk studies and is widely used in different atmospheric dispersion and emergency response research, e.g., [13], [14], and many others. However, despite such a wide use of puff models in practical and scientific applications, data assimilation methods with such models were rarely applied, especially in comparison with a number of applications of data assimilation to Eulerian ADMs. A few familiar to authors studies concerning data assimilation in puff models include [7],[15]-[17]. Another important motivation for the model choice is that computational algorithm of puff ADMs is in many respects close to that of Lagrangian ADMs, such as [10]. Since Lagrangian ADMs have advantages over the Eulerian ADMs in predicting atmospheric dispersion close to source, [18], development of data assimilation algorithms for them is a challenging task. However, stochastic nature of equations of particle movement must be addressed in order to apply data assimilation method developed here to Lagrangian ADM.

This work is an extension of the previous work [8] where data assimilation methodology has been developed for source function estimation in puff ADM. In the present work the variational approach to data assimilation in puff ADM is extended to deal with wind field estimation and the adjoint equations for puff ADM are derived. Since the numerical tests in the present work were performed for the case of two-dimensional wind field with zero vertical velocity, the statement of the problem and methodology are described for the case of 2D wind field, comprising only horizontal components. Results of numerical tests in idealized settings – constant wind speed and 2D flow – are presented.

2. Problem formulation

2.1 General

In puff ADM the continuous release of the pollutant is represented as a sequence of instantaneous releases –‘puffs’, (see, e.g., [23]). Each puff i is characterized by the coordinates of position-vector $\bar{r}_i = (x_i, y_i)^T$ (henceforth superscript “ T ” means transposition). In the considerations below the reference point of the Cartesian coordinate system is located at the ground level and horizontally coincides with the release location. The axes x, y are directed horizontally. Puffs are transported by the wind, hence the coordinates of the i -th puff are described by the differential equation: $d\bar{r}_i / dt = \bar{u}_p(\bar{r}_i)$, with initial condition $\bar{r}_i^T(t_i^0) = (0, 0)$, where $\bar{u}_p(\bar{r}_i) = (u_p(\bar{r}_i), v_p(\bar{r}_i))$, is the wind vector at the point of puff location, t_i^0 is time of release, $t_i^0 = i\tau$, τ is time interval between releases of puffs. As the wind field is given on the grid of MPP (vectors $\bar{u}, \bar{v} \in R^N$, $N = N_x N_y$, where N_x, N_y are grid dimensions in

x and y directions), some kind of interpolation is used to define velocity vector $\bar{u}_p(\bar{r})$ at the puff's location. Here the following $1/r^2$ interpolation scheme is used:

$$\begin{aligned}\bar{u}_p(\bar{r}) &= \tilde{f}(\bar{v}, \bar{r}_i) = (f(\bar{u}, \bar{r}_i), f(\bar{v}, \bar{r}_i))^T, \\ f(\bar{u}, \bar{r}_i) &= u_p(\bar{r}_i) = \frac{1}{W_i} \sum_{k=1}^N w_{ik} u_k, \\ w_{ik} &= \frac{1}{r_{ik}^2 + r_0^2}, \quad W_i = \sum_{k=1}^N w_{ik}, \quad r_{ik}^2 = (x_i - x_k^G)^2 + (y_i - y_k^G)^2\end{aligned}\quad (1)$$

where $\bar{v}^T = (\bar{u}^T, \bar{v}^T)$ is gridded wind field, u_k are the components of vector \bar{u} , the coefficients w_{ik} define the weight of the k -th grid node depending on its squared distance to the puff i , (x_k^G, y_k^G) are the coordinates of k -th grid node and r_0^2 is a small parameter to avoid discontinuity for zero distances. Thus, the equations of puffs' motion are:

$$d\bar{r}_i / dt = \tilde{f}(\bar{v}, \bar{r}_i). \quad (2)$$

Each puff is characterized by a Gaussian-shaped spatial distribution of matter due to turbulent diffusion. Then the matter concentration C at an arbitrary spatial point of the 3D domain (x, y, z) at time t is calculated as sum of contributions of all puffs:

$$\begin{aligned}C(x, y, z, t) &= \frac{1}{(2\pi)^{3/2}} \sum_{i=1}^{N_p} \frac{q_i \tau \cdot \gamma(t, \tau, i)}{\sigma_{xi} \sigma_{xi} \sigma_{zi}} \times \exp \left[-\frac{1}{2} \left(\frac{x_i - x}{\sigma_{xi}} \right)^2 \right] \\ &\times \exp \left[-\frac{1}{2} \left(\frac{y_i - y}{\sigma_{xi}} \right)^2 \right] \times \left\{ \exp \left[-\frac{1}{2} \left(\frac{H_i^{src} - z}{\sigma_{zi}} \right)^2 \right] + \exp \left[-\frac{1}{2} \left(\frac{H_i^{src} + z}{\sigma_{zi}} \right)^2 \right] \right\}\end{aligned}\quad (3)$$

Here N_p is the total (maximum) number of puffs, q_i is the release rate corresponding to the time interval of appearance of the i -th puff, H_i^{src} is release height of i -th puff, σ_{xi}, σ_{zi} are the parameters characterising the spatial distribution in the puff and the function $\gamma(t, \tau, i) = H(t - i \cdot \tau)$ is Heaviside step function which eliminates the influence of non-existing puffs. Total reflection of the cloud from the underlying surface is assumed in (3). Relationship (3) also assumes absence of deposition and reactions. In the present work σ_{xi}, σ_{zi} are parameterized by the Pasquill relationships, [23]:

$$\begin{aligned}\sigma_{x(z)i} &= b_{x(z)} l_i^{q_{x(z)}} \\ dl_i / dt &= (u^2(\bar{r}_i) + v^2(\bar{r}_i))^{1/2} = \tilde{f}(\bar{v}, \bar{r}_i),\end{aligned}\quad (4)$$

here l_i is travel distance of the puff and q_x, b_x, q_z, b_z are parameters depending on the release height and stability index. Consider the problem of modelling atmospheric dispersion on time interval $(0, T_f)$. Assume that during the

interval $(0, T), T < T_f$ measurements are available from K measurement stations located in spatial points $\bar{r}^k = (x^k, y^k, z^k)^T, 1 \leq k \leq K$. Assume also that the source of release acts during time interval $(0, T)$. Then in equation (1): $N_p = [T/\tau]$, where square brackets means taking an integer part. Denote concentration, measured at time t by the k -th station as $C_k^o(t)$. The available measurements during interval $(0, T)$ can be used to improve input parameters of the ADM and thus to improve the modeling results on the whole interval of calculations $(0, T_f)$. The adjustable parameters in the assimilation procedure compose the control vector $\bar{\psi}$ of size Ψ . In the present work special attention is given to two special cases of control vectors. In the first case only the source function is adjusted: $\bar{\psi}^T = (q_1, \dots, q_{N_p}) = \bar{q}^T, \Psi = N_p$, while in the second case the velocity field is adjusted and $\bar{\psi}^T = \bar{v}^T, \Psi = 2N$. In the third case which is considered in the present work both source function and wind field are adjusted and $\Psi = 2N + N_p$.

Now introduce the state vector of the model which consists of 2D position-vectors and travel distances of all puffs: $\bar{s}^T = (\bar{r}_1^T, l_1, \bar{r}_2^T, l_2, \dots, \bar{r}_{N_p}^T, l_{N_p}) \in R^{3N_p}$. Evolution of different components of the state vector is described by equation:

$$\frac{d\bar{s}}{dt} = \hat{f}(\bar{s}, \bar{v}), \quad (5)$$

where function \hat{f} is obviously constructed from abovementioned functions $\tilde{f}, \tilde{\tilde{f}}$ describing right parts in equations (2), (4) of puff's position vector, and travel distance change. Then (3) defines function $\tilde{C}(\bar{r}^k, \bar{s})$ giving the relationship between the state vector \bar{s} and the concentration at the measurement point k . The problem of data assimilation can be posed ([4]) as an optimal control problem of minimizing the following objective function with respect to control vector $\bar{\psi}$, subject to constraints which will be specified below:

$$\begin{aligned} J &= J_1 + J_2 \\ J_1 &= (\bar{\psi} - \bar{\psi}^B)^T \underline{\underline{B}}^{-1} (\bar{\psi} - \bar{\psi}^B) \\ J_2 &= \sum_{n=1}^{N_o} \sum_{k=1}^K \frac{1}{\sigma_o^2} \left(C_k^o(t_n) - \tilde{C}(\bar{r}^k, \bar{s}(t_n)) \right)^2 = \frac{1}{\sigma_o^2} \left(\bar{C}^o - \Omega(\bar{\psi}) \right)^T \left(\bar{C}^o - \Omega(\bar{\psi}) \right) \end{aligned} \quad (6)$$

Here $\bar{\psi}^B$ is first guess estimation of the control vector, $\underline{\underline{B}}$ is covariance matrix of the errors of the control vector, which everywhere below is assumed to be diagonal: $\underline{\underline{B}} = \text{diag}(\bar{\sigma}_B), \underline{\underline{\sigma}}_B = (\sigma_{1B}^2, \dots, \sigma_{\Psi B}^2)$, with σ_{iB}^2 being mean

squared error of the i -th component of first guess estimation of the control vector, σ_o^2 is mean squared error of the concentration measurements assumed to be constant, $N_o = T / \tau_o$ is number of time subintervals covering interval $(0, T)$ (τ_o is time interval between observations), vector $\bar{C}^o \in R^{N_o K}$ consists of concentrations $C^o(n, k)$, measured on each subinterval Δt_n by k -th station. The elements of C^o are ordered sequentially as follows: $C_l^o = C_{(n-1)K+k}^o = C^o(n, k)$. The corresponding vector that consists of the calculated concentrations at the K stations at the N_o time intervals (by model (3), (5)) is denoted by $\bar{C}^M = \Omega(\bar{\psi})$, where function Ω is formally introduced relating \bar{C}^M and $\bar{\psi}$. Error parameters entering (6) can reflect physical information concerning quality of measurements and of a priori information about background estimations of adjusted parameters. Alternatively when such estimations are not available they can become purely tuning parameters.

2.2 Source emission rate adjustment

In case of source function estimation ($\bar{\psi} = \bar{q}$), the dependence of both parts of function (6) on $\bar{\psi}$ is explicit and linear, therefore $\bar{C}^M = \underline{G}\bar{\psi} = \Omega(\bar{\psi})$, where elements of matrix \underline{G} are easily constructed from (3). Thus in case of $\bar{\psi} = \bar{q}$, the minimization of function (6) is a linear regression problem subject to constraints: $\bar{\psi} \geq 0$. Henceforth this is referred as “problem 1”. In case of problem 1, the corresponding background errors are assumed to be constant and denoted as: $\sigma_{iB}^2 = const = \sigma_{Bq}^2, \forall i : 1 \leq i \leq N_p$. Thus minimization problem solution depends in that case only on one parameter $\sigma^{-1} = \sigma_{Bq}^2 / \sigma_o^2$, which accounts for weight of regularization (background) term J_1 in (6).

2.3 Wind field adjustment

The case when $\underline{\psi}$ consists of wind field is referred below as “problem 2”. In this case the dependence of function $\tilde{C}(\bar{r}^k, \bar{s})$ on $\bar{\psi}$ is implicit, through dependence of the right parts of (5) on $\bar{\psi}$, describing evolution of the state vector components. Wind field which minimizes function (6) has to satisfy additional constraints. This now will be considered in more detail.

The atmospheric dispersion module of modern ERSs consists of two main parts: meteorological pre-processor (MPP) and ADM. The task of MPP is to calculate the gridded meteorological fields using input (a) prognostic meteorological fields calculated by Numerical Weather Prediction (NWP) models on a coarser grid and (b) observations. That problem is solved with the use of different physical parameterizations describing atmospheric processes together with linear interpolation and data assimilation algorithms [24], [20]. The meteorological fields calculated by MPP's are also subject to constraints, such as nondivergence of the flow field, [24], and/or linearized equations describing flow perturbations due to underlying topography [25]. In the present paper it is assumed that

the meteorological field was already calculated by MPP. However corrections to wind field due to assimilation of the concentration measurements are to be calculated and they have to satisfy the same relationships which are used by the meteorological pre-processors. The resulting gridded wind field $\bar{v}^T = (\bar{u}^T, \bar{v}^T)$ is to be non-divergent:

$$\underline{\underline{D}}\bar{v} = \underline{\underline{D}}\underline{\underline{v}} = 0$$

$$\left(\underline{\underline{D}}\bar{v}\right)_{l=(i-1)N_y+j} \approx \left(\frac{\partial u}{\partial x} + \frac{\partial v}{\partial y}\right)_{x=ih+x_{ori}, y=jh+y_{ori}}, \quad (7)$$

where $\underline{\underline{D}}$ is $N \times 2N$ matrix which approximates divergence operator at each node of the domain of calculations including boundaries, (i, j) are indices of the grid node in x, y directions respectively, (x_{ori}, y_{ori}) are coordinates of the lower-left corner of the grid and l is the row number.

The corrections $\delta u_i = u_i - u_{bi}, i=1,2$ to the first guess estimation of the wind field $u_{bi, i=1,2} = (u_b, v_b)$ induced by assimilation of concentration measurements are expected to be small in comparison with the magnitude of first guess estimation of wind velocity $U_b = (u_b^2 + v_b^2)^{1/2}$. Then linearized equations for perturbations of wind field used in some meteorological preprocessors (e.g., [25]) are valid and can be used as additional linear constraints on the minimization problem. For the case of horizontal 2D flows equations from [25] are reduced to: $u_b (\partial \delta u_i / \partial x) + v_b (\partial \delta u_i / \partial y) = (\rho^{-1}) (\partial \delta p / \partial x_i)$, where $i=1,2$, $x_1 = x, x_2 = y$, ρ is density and δp - pressure perturbation. After standard rearrangements to exclude pressure perturbations this gives:

$$\frac{\partial}{\partial y} u_b \frac{\partial u}{\partial x} + \frac{\partial}{\partial y} v_b \frac{\partial u}{\partial y} - \frac{\partial}{\partial x} u_b \frac{\partial v}{\partial x} - \frac{\partial}{\partial x} v_b \frac{\partial v}{\partial y} = \frac{\partial}{\partial y} u_b \frac{\partial u_b}{\partial x} + \frac{\partial}{\partial y} v_b \frac{\partial u_b}{\partial y} - \frac{\partial}{\partial x} u_b \frac{\partial v_b}{\partial x} - \frac{\partial}{\partial x} v_b \frac{\partial v_b}{\partial y}. \quad (8)$$

Equation (8) is approximated inside domain of calculations except boundaries and then can be written:

$$\underline{\underline{W}}\bar{v} = \underline{\underline{W}}\underline{\underline{v}}_b, \quad (9)$$

Here elements of $(N_x - 2)(N_y - 2) \times 2N$ matrix $\underline{\underline{W}}$ can be easily specified in accordance to numerical approximation scheme.

Thus, problem 2 of wind field correction with concentration measurements can be posed as problem of minimizing function (6) with respect to $\bar{v} = \bar{v}^T$ subject to linear constraints (7), (8).

3. Solution methodology

Since as problem 1 of source emission rate correction with assimilation measurements is a linear regression problem, a variety of methods can be used for its solution. Here subroutine “lsqnonneg” from Matlab 7.0 Optimization Toolbox was used, which finds the nonnegative solution that minimizes function (6) using an algorithm described in [26].

In case of problem 2, which is linearly constrained minimization; subroutine “fmincon” from MATLAB 7.0 Optimization Toolbox was used, which in case of large scale optimization problem uses a subspace trust region method. It is based on the interior-reflective Newton method described in [27] and [28]. In each iteration an approximate solution of a large linear system is obtained using the preconditioned conjugate gradients method. Termination conditions are: $\|\bar{\psi}^{s+1} - \bar{\psi}^s\| < TolX$, $|J^{s+1} - J^s| < TolF$, in which $TolX$, $TolF$ are termination tolerances for control vector and cost function respectively and s is iteration number. Values $TolX = TolF = 10^{-12}$ were used everywhere in the present study. An important practical feature of this subroutine is that it can use matrices representing constraints in (7) and (9) stored in sparse format. The algorithm requires gradient of function (6) with respect to $\bar{\psi}$ and approximation of nonzero stencil for Hessian matrix for approximate Hessian calculations. The nonzero stencil for Hessian (i.e. set of indices, for which elements of Hessian are assumed to be nonzero) is specified as: $Stenc = \{i, j : j = i \vee j = i \pm 1 \vee j = i \pm N_y\}$. Thus diagonal of Hessian is assumed to be nonzero together with those elements which correspond to linking of the l -th node of computational grid ($l = (i-1)N_y + j$) with the neighbour nodes.

Gradient $\partial J_1 / \partial \bar{\psi}$ of first term in right part of function (6) is calculated straightforwardly. Second term of (6) is approximation of integral: $J_2 \approx \frac{1}{\tau_o} \int_0^T \sum_{k=1}^K \frac{1}{\sigma_o^2} \left(C_k^o(t) - \tilde{C}(\bar{r}^k, \bar{s}(t)) \right)^2 dt = \int_0^T \Phi(\bar{s}) dt$. Therefore, following classical optimal control theory, (e.g., [29]), $\partial J_2 / \partial \bar{\psi}$ can be calculated with the use of adjoint equations:

$$\frac{d\varphi}{dt} + \hat{f}_{\bar{s}}^T \varphi = -\Phi_{\bar{s}}(t), \quad \varphi(T) = 0. \quad (10)$$

Here vector φ of size $3N_p$ is solution of adjoint system of equations, $\Phi_{\bar{s}} = \left(\Phi_{s_1}, \dots, \Phi_{s_{3N_p}} \right)$, $\hat{f}_{\bar{s}}$ is Jacobi matrix of function \hat{f} from (5), which is calculated by differentiating the relationships (1). Note that, due to the fact that puffs are not interacting, $\hat{f}_{\bar{s}}$ has block structure with each block of size 3×3 . Hence, solution of (10) can be performed separately for each block (each puff). Then gradient $\partial J_2 / \partial \bar{v}$ is calculated from the relationship (which takes into account also stationarity of the velocity field):

$$\frac{\partial J_2}{\partial \bar{v}} = \int_0^T \hat{f}_{\bar{v}}^T(t) \varphi(t) dt. \quad (11)$$

In (11) $\hat{f}_{\bar{v}}$ is Jacobi matrix of function \hat{f} from (5), considered as a function of the velocity field, which is also calculated by taking appropriate derivatives of relationships (1). All Jacobi matrices in (10), (11) are to be calculated on puff trajectories from forward model run. Hence, in calculating the derivative $\partial J / \partial \bar{\psi}$, during

forward run of the model (i.e., solution of equation (5) for state vector and concentration calculations with (3)), the right part for adjoint equations $\Phi_{\bar{s}}$ is calculated, puff's trajectories are stored, and in backward run adjoint equations are solved and gradient itself is calculated. Discretizations of (10), (11) are performed following the approach from [4] (Chapter 21), so that the resulting solution gives gradient of discretized cost function (6).

When control vector $\bar{\psi}^T = (\bar{q}^T, \bar{v}^T)$ consists of both – source function components and velocity field, the problem of minimization of cost function (6) (problem 3) is solved in the following iteration process:

$$\begin{aligned}
 & s = 0; \bar{q} = \bar{q}^b; \bar{v} = \bar{v}^b; \\
 & \text{while } (s < s_{\max}) \text{ do} \\
 & \quad s = s + 1; \\
 & \quad \text{solve problem 1; update } \bar{q}; \\
 & \quad \text{solve problem 2; update } \bar{v}; \\
 & \text{enddo}
 \end{aligned} \tag{12}$$

Thus in the overall minimization procedure problems 1 and 2 are solved by turns. Iteration process (12) is sort of descent algorithm and always converges to stationary point. However, convergence of (12) to global solution of the problem 3, as well as convergence of fmincon to global solution of problem 2 are not guaranteed as far as cost functions are non-convex in those cases.

Note, that presented statement of the problem considers simple puff model. In more complex puff models, such as [12] turbulent dispersion of matter is accounted by solving separate equations for $\sigma_x, \sigma_y, \sigma_z$ instead of parameterization (4). The presented statement of the problem and solution methodology could be straightforwardly applied for such cases by including $\sigma_x, \sigma_y, \sigma_z$ in state vector \bar{s} instead of puff travel distance.

4. Calculation results

In this section results of two calculation cases are presented. In the first case wind velocity was considered as constant in space, i.e., the velocity field was not specified on the grid, but was represented by 2 parameters - u and v components of wind vector. All derivations from the previous section are applicable to that case when $N = 1$ (thus, dimension of control vector $\bar{\psi}$ in problem 2 is 2). This case is important, since it most clearly demonstrates the importance of the wind vector correction for better estimation of the source function. In the second case, which is much more complex than the first due to the problem size, the correction of 2D wind field is considered.

In all cases the so-called “identical twin” experiments ([32]) have been used to evaluate the performance of the data assimilation methodology, due to lack of real experimental data. Artificial “concentration measurements” have been generated by running the model with a source term and a wind field that are considered as “true” (the “truth” run). Then the model was run again (assimilation run), assuming that the source term and wind field are unknown. “First guesses” of the source term and wind field were used and the previously generated artificial

concentration measurements were assimilated, with the aim to evaluate the “true” parameters. Particular details of each test case are given below. In addition, to overcome the tendency of identical twin experiments to err on the optimistic side ([32]), the observation error has been simulated by adding noise to the synthetic observations.

4.1 Results with constant wind speed

In that case the true values of the velocity components in all runs were the same: $u^{true} = 10 \text{ m/s}$, $v^{true} = 0$. Runs with different true source functions had been performed. The release duration in all cases was: $T = 1h$. The modelling duration in all cases was: $T_f = 2h$. Three variants of source functions were considered. The first and second true source functions were constant: $q^{1true}(t) = 10^6 \text{ Bq/s}$, $q^{2true}(t) = 10^8 \text{ Bq/s}$. The third true source function first linearly diminished from $q^{3true}(0) = 10^7 \text{ Bq/s}$ to $q^{3true}(T/4) = 10^6 \text{ Bq/s}$, then linearly increased to $q^{3true}(3T/4) = 10^8 \text{ Bq/s}$, and then again linearly diminished to the initial value: $q^{3true}(T) = q^{3true}(0) = 10^7 \text{ Bq/s}$. The first guess estimation of the wind velocity in assimilation runs was the following: $u^{0guess} = 7 \text{ m/s}$, $v^{0guess} = 2 \text{ m/s}$. In all cases the first guess of the source function was the same: $q^{0guess}(t) = 10^7 \text{ Bq/s}$. Thus, it differed by an order of magnitude from the all three kinds of true source functions. Such errors in source function and wind estimations are realistic in operational practice of real-time ERSs, [2]. Note, that despite the fact, that q^{1true} , q^{2true} were constant functions, in the assimilation run that information was not available, i.e., source function was not described by one parameter, but was approximated by the vector of the size N_p . The coordinates of the measuring stations (i.e., points, from which output from the truth runs was used in assimilation runs) were situated at the level $z = 0$, and had the following horizontal coordinates: $(x^{1out}, y^{1out}) = (10^4 \text{ m}, 0)$, $(x^{2out}, y^{2out}) = (7071 \text{ m}, 7071 \text{ m})$, $(x^{3out}, y^{3out}) = (7071 \text{ m}, -7071 \text{ m})$. For each truth run a series of assimilation runs have been performed with different values of σ . The best value of the regularization parameter σ in operational practice, when true concentration field is unknown can be calculated by heuristics techniques, such as [30]. However trial and error was used in the present study to find the best value of σ because true concentration field was known and because it is easier by computational time. The time interval between measurements was: $\tau_0 = 600 \text{ s}$. Other parameters were the same in truth and assimilation runs: $x_0 = y_0 = 0$, $H_i^{src} = 10 \text{ m}$, $\forall i: 1 \leq i \leq N_p$, $\tau = 300 \text{ s}$, $p_x = 1.503$, $q_y = 0.833$, $p_y = 0.151$, $q_z = 1.219$.

The quality of the results was evaluated by the normalized mean square error ($NMSE$) and fractional bias (FB), calculated with the use of output concentration fields (in truth and assimilation runs) on the computational grid, which covered spatial-time domain $(0 \leq x \leq 30 \text{ km}) \times (-20 \text{ km} \leq y \leq 20 \text{ km}) \times (0 \leq t \leq 2h)$ with spatial horizontal

steps 1km , and with time step 600 s. In total more then 4000 values were used for comparisons of truth and assimilation runs, while only from 6 to 18 measured values were used in assimilation procedure. Thus evaluation was based on global error indicators.

Table 1 presents minimum by σ achieved calculated values of *NMSE* and *FB* for different assimilation series (cases). Brief description of each case is given in column ‘description’ of the Table 1. In cases 1-3 wind velocity in assimilation run was equal to the true value. Therefore, the errors obtained in those cases were much less then the errors in more complex cases 4-9, when initial wind velocity was erroneous. Results of cases 4-5, 6-7, 8-9 show the influence of adjustment of wind velocity on the accuracy of the results. In all cases 5, 7,9, *NMSE* with adjustment of wind velocity together with source function is by the factor of 2-200 less then *NMSE* in cases 4, 6, 8, with adjustment of the only source function. In the majority of cases *FB* also diminishes with adjustment of wind velocity, though its reduction is not so significant as that of *NMSE* .

Fig. 1 shows example of source functions – true, first guess and adjusted for cases 8 and 9. The effect of the wind speed correction in assimilation procedure on the adjustment of the source function is evident, which confirms results following from Table 1. Similar pictures were obtained for the rest of the runs.

4.2 Results with two dimensional flow

Common parameters of truth and assimilation runs were the following. Velocity field was calculated on the grid with $N = N_x \times N_y = 40 \times 40$ cells covering spatial domain $(0 \leq x \leq 40km) \times (-40km \leq y \leq 40km)$ with spatial horizontal steps 2x2 km. The release duration was $T = 1h$. Model equations (5) were integrated with time step $\tau_m = 100s$ and concentrations calculated with the same time step $\tau_o = \tau_m$. Other parameters were the following: $H_i^{src} = 10m$, $\forall i : 1 \leq i \leq Np$, $p_y = 1.503$, $q_y = 0.833$, $p_z = 0.151$, $q_z = 1.219$.

The truth run in that case was characterized by the following conditions. Wind field was characterized by rotation around point with coordinates $r^0 = (x^0, y^0) = (0, -5 \cdot 10^4 m)$ with angular velocity $\omega = 2 \cdot 10^{-4} 1/s$, so that: $u^{true}(x, y) = \omega(y - y^0)$, $v^{true}(x, y) = -\omega(x - x^0)$. At the point of release, the wind was blowing in x direction with magnitude $10 m/s$, and the resulting vector field is presented at Fig. 2-a.

The assimilation runs were characterized by the following conditions. The modelling duration was $T_f = 2h$. The first guess wind field (Fig. 2-b) was constant in space and was equal to true wind vector in the point of release: $u^{0guess}(x, y) = u^{true}(0, 0)$, $v^{0guess}(x, y) = v^{true}(0, 0)$. This condition reflects the fact, that in operational practice of many ERSs meteorological measurements are usually available at the point of potential release. That information can be used by meteorological pre-processors together with NWP data in data assimilation procedure, to

construct the wind field, which can be locally very close to the observed, [20]. However the overall error of such constructed first guess wind field in present case was quite large. The so-called ‘vector wind difference’ error indicator was used for estimation of the wind field error, which simultaneously reflects error in magnitude and in wind direction, [31]:

$$vwd = \left\langle \left((u - u^{truth})^2 + (v - v^{truth})^2 \right)^{1/2} \right\rangle, \quad (13)$$

where triangular brackets indicate arithmetic average. Thus, error of first guess wind field was: $vwd^{0guess} = 6 \text{ m/s}$ which is comparable to errors, that can occur in operational meteorological practice [31].

The measurement points were located at three concentric circles around the release point with radiuses $R_1^m = 5\text{km}$, $R_2^m = 10\text{km}$, $R_3^m = 30\text{km}$ and at each circle they were distributed with uniform angular step $\delta\phi$ which varied in different tests from 3° to 30° starting from 0° direction, which coincided with positive direction of axis x .

The following errors parameters of function (6) were set in all cases. Parameter σ_0^2 in all cases was set to $\sigma_0^2 = 10^{-5}$. In case of adjustment of wind field (problem 2) error of the background field $\bar{\sigma}^B = \bar{\sigma}^{Bu}$ was defined by the following relationship: $1/\sigma_{Bu}^2 = (1/\sigma_{uobs}^2) \exp(-R_l^2 / R_{infl}^2) + (1/\sigma_{u0}^2)$. Here the first term accounts for decrease of error closer to observation (release) point, R_l is distance from l -th grid node to release point, R_{infl} is radius of influence of wind observation, which was taken $R_{infl} = 5\text{km}$, σ_{uobs}^2 is squared error of observation assumed to be small enough to nudge velocity in the release point to measured value ($\sigma_{uobs}^2 = 10^{-4} \text{ m}^2 / \text{s}^2$) and σ_{u0}^2 is squared error of background field uninfluenced by observation (far from release point) which varied in different tests. When source function was adjusted, parameter σ_{Bq}^2 was set to zero.

In the same way as in section 4.1 results of assimilation were evaluated by global error estimations - $NMSE$ and FB which were calculated on the basis of truth and predicted concentrations on the spatial grid, coinciding with the velocity grid and with temporal resolution coinciding with model integration step. Thus in total about $5 \cdot 10^4$ values were used in $NMSE$ calculations.

Consider first special case, when only wind field was adjusted. Source function in that case was constant $q^{0guess}(t) = q^{true}(t) = 10^7 \text{ Bq/s}$. Results of the corresponding tests are presented in Table 2. Fractional bias error of first guess and assimilation runs in all tested cases was small ($FB < 10^{-2}$) and thus is not presented. The run with first guess estimation of velocity field led to $NMSE^{0guess} = 1.3$, $VWD^{0guess} = 6 \text{ m/s}$. As it can be seen from Table 2, despite the fact, that source function was known, it is rather difficult to find minimum of cost function due to very high dimension of the problem, and convergence to good solution was possible only when both constraints

(7) (non-divergence) and (8) (linearized flow) were used. In contrast, when constraints were not used (case 3) or when only non-divergence constraint was used (case 2) final analyzed velocity and concentration fields were worse than first guess estimation (VWD and $NMSE$ increase). As follows from case 4, the quality of the first guess velocity field is crucial for finding an appropriate solution. When error of the background field was very large, algorithm converged to completely inappropriate solution with $VWD = 500$, though in that case not only cost function was reduced, but even global error estimate $NMSE$ was essentially reduced by the factor of 10. Cases 5-7 demonstrate sensitivity of the results with respect to angular resolution of observation network. With decreasing the resolution (increasing $\delta\phi$ from 3° to 30°) improvement in both, $NMSE$ and FB was reached, however effectiveness of assimilation ζ^{nmse} measured as relative decrease: $\zeta^{nmse} = NMSE^{0guess} / NMSE^{assim}$ fell from 65 to 2.6. Effectiveness ζ^{vwd} , measured as $\zeta^{vwd} = VWD^{0guess} / VWD^{assim}$ decreased significantly slower from 1.4 to 1.13. Such behaviour can be attributed to the fact that $NMSE$ is most sensitive to errors in velocities close to the source of release, where concentrations are larger. From the other hand the fact that values of ζ^{vwd} are significantly lower than ζ^{nmse} demonstrates high sensitivity of $NMSE$ to accuracy of velocity field.

Figures 2 and 3 presents wind vectors and concentration distributions in true run, in first guess run and in assimilation run (case 1 from Table 2). The effect of data assimilation on both distributions is evident from these Figures. An interesting feature observed from Figures 2 and 3 is that velocity field is modified not only in the area of presence of cloud, but in the entire domain, even in the areas outside the cloud extent. This is possible only due to the influence of constraints (7), (8).

Now consider the more complex problem, when both source function and wind field are unknown. Conditions of all experiments were almost the same as in previous case. The following true source functions $q^{true}(t)$ were used. At zero time: $q^{true}(0) = 10^7 Bq/s$, then it linearly increased to: $q^{true}(T/4) = \alpha q^{true}(0)$, then it linearly decreased to $q^{true}(3T/4) = (1/\alpha)q^{true}(0)$, and then again linearly increase to the initial value: $q^{true}(T) = q^{true}(0)$. First guess source function was constant and equal: $q^{0guess}(t) = q^{true}(0)$. Cases with $\alpha = 10$ and $\alpha = 2$ were considered. In that series of experiments the ‘measured’ concentrations were perturbed with white Gaussian noise to account for measurement uncertainty. Squared standard deviation of Gaussian distribution was equal to abovementioned assumed mean squared error of observations σ_o^2 . Results of assimilation of both perturbed and unperturbed concentrations are presented in Table 3. As it can be seen from Table 3, perturbation of concentration measurements with Gaussian noise didn’t essentially influence the results of assimilation. When angular resolution of observation network was coarse ($\delta\phi = 30^\circ$) in both cases - $\alpha = 10$ and $\alpha = 2$ decrease in

$NMSE$ was reached while VWD increased. Increase in VWD occurred because relatively small errors in adjusted source function (Figure 4) lead to incorrect adjustment of velocity field. Thus improvement in $NMSE$ was reached due to adjustment of source function only. However, when angular resolution of observation network was sufficiently small ($\delta\phi \leq 15^\circ$) for both $\alpha = 10$ and $\alpha = 2$ decrease in both concentration errors $NMSE$ and wind field error VWD was reached.

5. Conclusions

In present work the methodology of combined adjustment of source function and wind field inputs of the puff Atmospheric Dispersion Model (ADM) through data assimilation of concentration measurements has been developed. Variational approach to data assimilation problem was adopted, in which cost function, characterising difference of predicted and measured concentrations was minimized with respect to either wind field and source function. Resulting wind field solution is subject to linear equality constraints following from nondivergence and linearized flow conditions. Adjoint equations for puff ADM are derived and solved numerically to find gradient of cost function with respect to wind field. The minimization problem is solved with the use of Matlab 7.0 Optimization Toolbox.

‘Identical twin’ numerical experiments have been performed for two kinds of idealized conditions: 1) case of constant in time and in space wind velocity (0D wind field); and 2) case of 2D wind field. After truth run had been performed, errors in source function and/or wind field had been introduced in first guess run. The error of first guess source function varied from zero to 1000% with respect to true source function. Vector wind difference error (VWD) of wind field was 3.6 m/s in first case and 6 m/s – in second. Those errors then had been reduced through the data assimilation procedure.

Results of the first case show very essential increase of accuracy of the resulting concentration field when wind velocity was corrected together with source function in comparison with the case when only source function had been corrected. Resulting normalized mean square error $NMSE$ reduced by the factor of from 2 to 200 under the influence of wind field correction. Second case was much more complex in comparison to the first one due to essential increase in the size of minimization problem (by 3 orders of magnitude). Two main sets of numerical tests were performed in the second case. In the first set true source function was known and only wind field was adjusted, while in the second set both source function and wind field were adjusted.

It was found that decrease in wind field error is possible only when suitable set of constraints is used (both non-divergence and linearized flow relationships). When constraints were not used, or when only non-divergence constraint was used improvement in wind field error was not possible. Quality of the first guess wind field was crucial for wind field correction, especially in the vicinity of release, where concentrations are large. When large

error of first guess wind field was assumed, correction was also not possible. Provided that the abovementioned conditions were fulfilled in tests with known source function VWD reduced by about $1.7 \div 0.7$ m/s and $NMSE$ - by a factor $65 \div 2.6$ depending on angular resolution of the observational network, which varied from 3 to 30 decimal degrees. In the second set of tests, when relatively large errors (by a factor of 10) in source function were introduced level of reduction of $NMSE$ was in all cases very large (by a factor of >100) due to adjustment of source function. However reduction of VWD in that case by about $1.7 \div 1.1$ m/s was achieved for angular resolutions of observational network: $3^\circ \leq \delta\phi \leq 15^\circ$. For larger angular resolution ($\delta\phi = 30^\circ$) VWD increased.

The presented methodology can be extended to cope with more realistic 3D flows and also for other kinds of problems, such as source location and plume rise estimations. Of course more tests will be needed in such cases.

6. Acknowledgements

The present work has been supported through the NATO reintegration grant NUKR.RIG.982362 "Atmospheric Pollution Data Assimilation for Emergency Response". Authors are grateful to Editor and anonymous referees for their useful comments.

References

1. Raskob W. European approach to nuclear and radiological emergency management and rehabilitation strategies (EURANOS). *Kerntechnik* 72 (4) (2007) 172-175.
2. Sjoreen A.L., et.al. Rascal Version 2.1 User's Guide NUREG/CR-5247. U.S. Nuclear Regulatory Commission, Washington, 1994.
3. Rojas-Palma C., et.al. Data assimilation in the decision support system RODOS. *Radiation Protection Dosimetry* 104 (2003) 31-40.
4. Dhall J.M., Lewis S., Lakshmivaran, S. D. Dynamic Data Assimilation: A Least Squares Approach. Cambridge University Press, 2006. – 655 p.
5. Enting I.G. Inverse Problems in Atmospheric Constituent Transport. Cambridge University Press, UK, 2002.
6. Quelo D., Sportisse B., Issnard O. Data assimilation for short range atmospheric dispersion of radionuclides: a case study of second-order sensitivity. *J. of Environmental Radioactivity* 84 (2005) 393-408
7. Krysta M., Bocquet M., Sportisse B., Isnard O., 2006. Data assimilation for short-range dispersion of radionuclides: An application to wind tunnel data. *Atmospheric Environment* 40, p. 7267-7279
8. Tsiouri V., et.al. Development and first tests of data assimilation algorithm in Lagrangian puff atmospheric dispersion model. Proc of Int. Conf HARMO 11, Cambridge, 2-5 July 2007, p. 182-186

9. Mikkelsen, T., Thykier-Nielsen, S., Hoe, S., 2007. Medium range puff growth. *Developments in Environmental Science*, Chapter 2.16, (6), pp. 243-252
10. Davakis E., Bartzis J.G. and Andronopoulos S. DIPCOT: A Lagrangian model for atmospheric dispersion over complex terrain. RODOS Report No RODOS(WG2)-TN(99)-01, (available from www.rodos.fzk.de)
11. Sørensen, J.H., Baklanov, A., Hoe, S., 2008. The Danish emergency response model of the atmosphere (DERMA). *Journal of Environmental Radioactivity* 96 (1-3), pp. 122-129
12. Scire J.S. Strimaitis D.G., Yamartino R.J., 1998. A user's guide for the CALPUFF dispersion model (Version 5). Earth Tech. Inc., Concord, MA (<http://www.src.com/calpuff/calpuff1.htm>)
13. Gilliam, R.C., Huber, A.H., Raman, S., 2005. Metropolitan-scale transport and dispersion from the New York World Trade Center following September 11, 2001. Part II: An application of the CALPUFF plume model. *Pure and Applied Geophysics* 162 (10), pp. 2005-2028
14. Barsotti, S., Neri, A., Scire, J.S., 2008. The VOL-CALPUFF model for atmospheric ash dispersal: 1. Approach and physical formulation. *Journal of Geophysical Research B: Solid Earth* 113 (3), art. no. B03208
15. Eleveld, H., Kok, Y.S., Twenhöfel, C.J.W., 2007. Data assimilation, sensitivity and uncertainty analyses in the Dutch nuclear emergency management system: A pilot study. *International Journal of Emergency Management* 4 (3), pp. 551-563
16. Cheng, Y., Reddy, K.V.U., Singh, T., Scott, P., 2007. CBRN data fusion using puff-based model and bar-reading sensor data. *FUSION 2007 - 2007 10th International Conference on Information Fusion*, art. no. 4408018
17. Anke Beyer-Lout, Young G.S., Haupt S.E., 2008. Concentration assimilation into wind field models for dispersion modelling. 15th Joint Conference on the Applications of Air Pollution Meteorology with the A&WMA (available from <http://ams.confex.com/ams/pdfpapers/132516.pdf>).
18. Nguyen, K.C., Noonan, J.A., Galbally, I.E., Physick, W.L., 1997. Predictions of plume dispersion in complex terrain: Eulerian versus Lagrangian models. *Atmospheric Environment* 31 (7), pp. 947-958
19. Davakis S., et. al., Data assimilation in meteorological pre-processors: effects on atmospheric dispersion simulations. *Atmospheric Environment* 41 (2007) 2917-2932.
20. Kovalets I., et.al. Introduction of data assimilation procedures in the meteorological pre-processor of atmospheric dispersion models used in emergency response systems. *Atmos. Env.* 38/3 (2004) 457-467
21. Daley R. Estimating the wind field from chemical constituent observations: experiments with a one dimensional extended Kalman filter. *Monthly Weathe Review* 123 (1995) 181-198.
22. Stuart A.L., et.al. Ensemble-based data assimilation and targeted observation of a chemical tracer in a sea breeze model. *Atmos. Env.* 41 (2007) 3082-3094

23. Thykier Nielsen S., Deme S., Mikkelsen T., Description of the Atmospheric Dispersion Module RIMPUFF. RODOS report WG2_TN98_02 (1998) (<http://www.rodos.fzk.de>)
24. COST Action 710 Final report. Harmonisation of the pre-processing of meteorological data for atmospheric dispersion models. Fisher B.E.A., et al. (eds.), L-2985 European Commission, Luxembourg, (1998)
25. Dunkerley F., et.al. LINCOM Wind Flow Model: Application to Complex Terrain With Thermal Stratification. Phys. Chem. Earth (B). 26(10) (2001) 839-842
26. Lawson, C.L. and Hanson R.J. Solving Least-Squares Problems, Prentice-Hall, Chapter 23, p. 161, 1974.
27. Coleman, T.F. and Li Y. An Interior, Trust Region Approach for Nonlinear Minimization Subject to Bounds. SIAM J. on Optimization 6 (1996) 418-445.
28. Coleman, T.F. and Li Y. On the Convergence of Reflective Newton Methods for Large-Scale Nonlinear Minimization Subject to Bounds. Mathematical Programming. 67 (1994) 189-224.
29. Fedorenko R.P., Approximate Solution of Optimal Control Problems. Nauka, Moscow, 1978 (in Russian).
30. Wahba G., Wendelberger J. Some new mathematical methods for variational objective analyses using splines and cross-validation. Monthly Weather Review 108 (1980) 1122-1143.
31. Stauffer D.R., and Seaman N.L. Use of four-dimensional data assimilation in a limited area mesoscale model. Part I. Monthly Weather Rev. 118 (1990) 1250-1277.
32. Daley, R., Atmospheric Data Analysis, Cambridge University Press, p.339, 1991

Abbreviated title

Improvement of source and wind field input of ADM

Figure captions

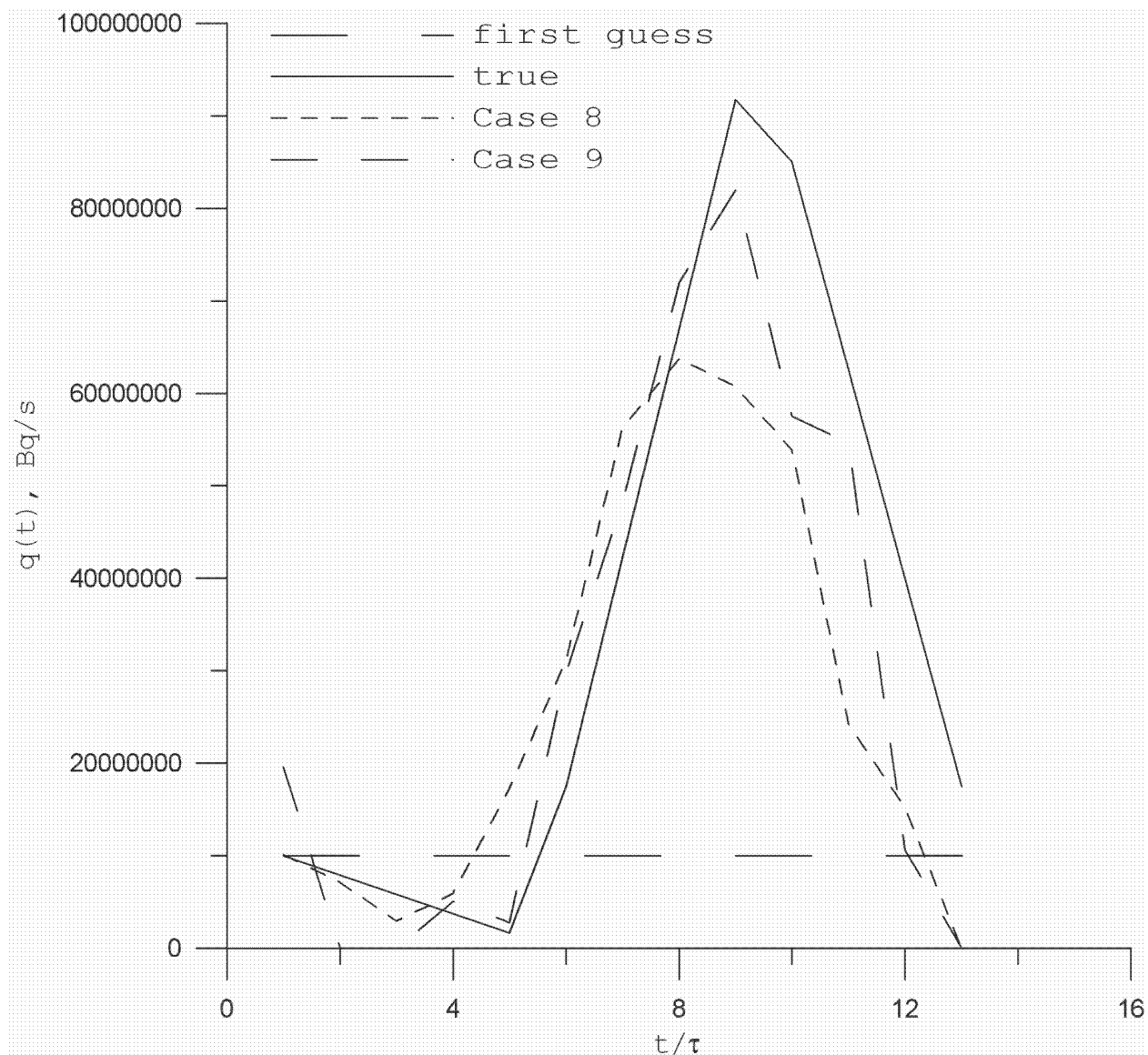


Figure 1. Source functions: true, first-guess and after assimilation runs. Case numbers correspond to the column 'N°' of the Table 1. Case N° 8 correspond to adjustment of source function only; case N° 9 – to adjustment of both source function and wind velocity components.

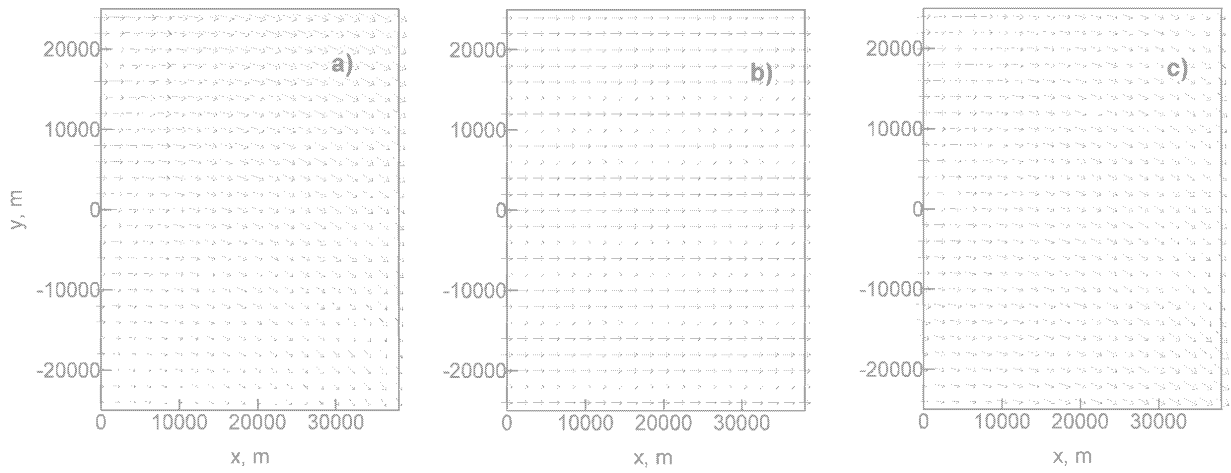


Figure 2. Velocity fields: a) true; b) first-guess; c) after assimilation run (case 1 of Table 2). Length of arrow is proportional to magnitude of velocity. True velocity in the point of release – 10 m/s.

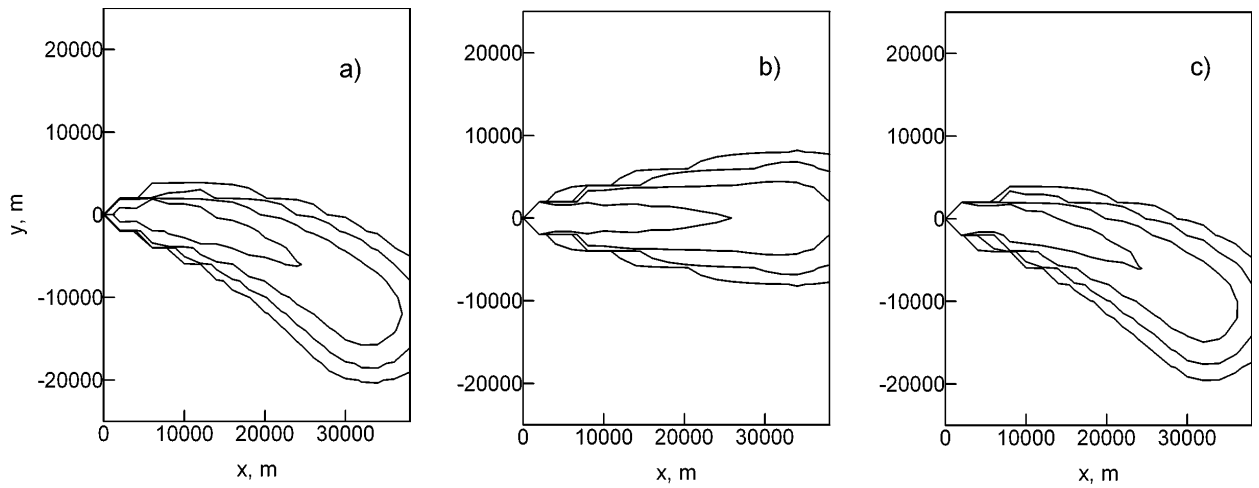


Figure 3. Near – ground concentration distributions after 1 hour after start of release: a) true; b) first guess; c) after assimilation run (case 1 of Table 2). Isolines of concentrations correspond to: 10^{-4} Bq/m³, 10^{-3} Bq/m³, 10^{-2} Bq/m³, 10^{-1} Bq/m³.

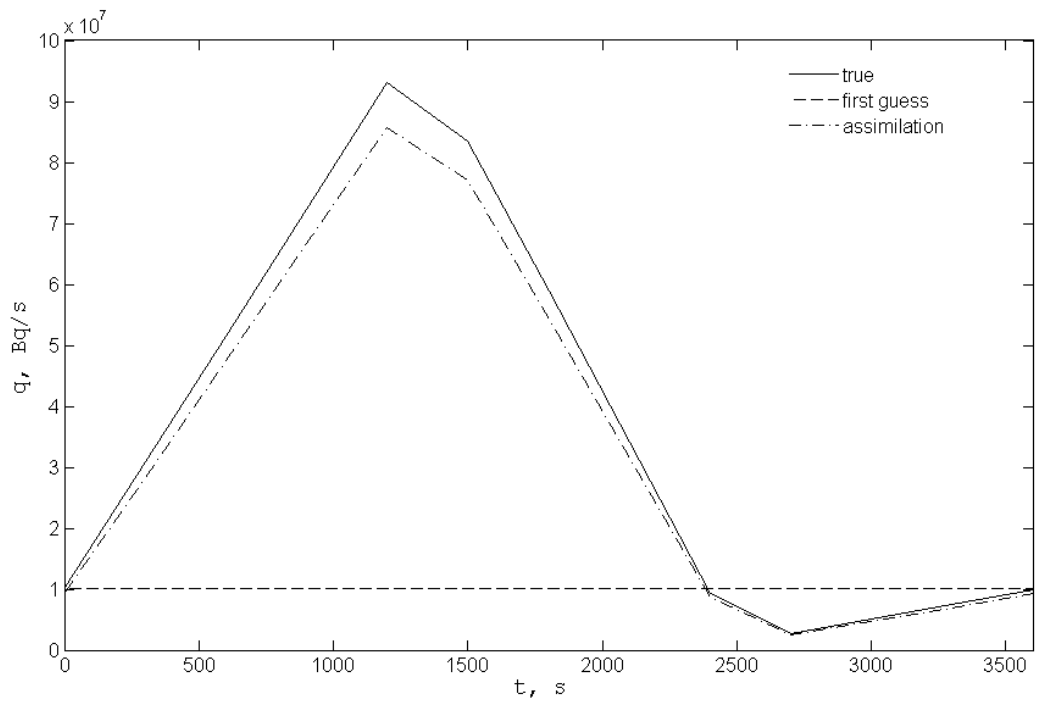


Figure 4. Source functions: true, first guess and after assimilation run in case 4 of Table 3.